ADVANCED MATERIALS TECHNOLOGIES
www.advmattechnol.de

Combustion-Assisted Photonic Sintering of Printed Liquid Metal Nanoparticle Films

*Shay Goff Wallace, Nathan P. Bradshaw, Nicholas X. Williams, Justin H. Qian, Karl W. Putz, Christopher E. Tabor, and Mark C. Hersam**

Liquid metals are ideally suited for flexible and wearable electronics due to their compatibility with additive manufacturing and high electrical conductivity that is maintained following mechanical perturbation. While printing of eutectic gallium–indium (eGaIn) liquid metal nanoparticles has been demonstrated, previous techniques for activating electrical conductivity in the as-printed insulating eGaIn nanoparticles limit throughput in roll-to-roll manufacturing processes. Here, ultrafast photonic sintering of eGaIn nanoparticles is demonstrated, which is further enhanced through the use of nitrocellulose as a carrier polymer that undergoes optically triggered combustion to produce eGaIn thin films with electrical conductivities exceeding 10^4 S cm^{-1}. This combustion-assisted photonic sintering (CAPS) is two orders of magnitude faster than previously demonstrated noncontact sintering techniques. By circumventing the established tradeoff between electrical conductivity and activation speed, CAPS will facilitate the use of eGaIn liquid metal nanoparticles in high-throughput additive manufacturing of flexible and wearable electronics, sensors, and related technologies.

1. Introduction

The field of printed electronics has attracted significant attention in recent years due to its potential for low-cost biomedical devices, wearable technologies, and sensors for the internet of things (IoT). Liquid metal (LM), such as eutectic gallium-indium (eGaIn), is ideally suited for use in flexible electronics since LM films can stretch and flex without degrading high electrical conductivity, making it a key component of applications ranging from batteries to antennae to reconfigurable electrical interconnects.[1–3] LM is patterned for electronic applications through a variety of means, including direct extrusion or injection,[2,4–6] selective wetting,[7] mechanical rupture of deposited nanoparticles,[8–10] and laser rupture of nanoparticles.[11,12] While these techniques produce robust, high-performance LM films, they are relatively low-throughput processes, which has limited the use of LM in roll-to-roll manufacturing.

While direct deposition of bulk eGaIn has been demonstrated, the spontaneous formation of a gallium oxide skin on the surface of eGaIn results in a high surface tension that is incompatible with commonly used liquid processing methods and printing techniques (e.g., inkjet printing).[13–17] Colloidal dispersions of eGaIn mitigate these limitations by breaking the eGaIn into nanoparticles where the fluid properties are instead dictated by the surrounding liquid. In this manner, the surface tension and viscosity of eGaIn nanoparticle dispersions can be optimized for a variety of printing techniques that are incompatible with bulk eGaIn.[13,17] However, the spontaneous formation of electrically insulating surface gallium oxide also presents challenges for manufacturing electronics using eGaIn nanoparticles, because additional processing is required after printing to rupture the oxide shell and achieve an electrically conductive percolating network. Bulk eGaIn does have the advantage of not requiring this sintering process, but its material characteristics prevent it from being used in rapid roll-to-roll manufacturing environments that require repeatability and scalability.[13]

The eGaIn nanoparticle sintering process is typically performed through direct mechanical contact stress-induced fracture or indirectly through heating the metallic core with a laser, which results in shell fracture due to a mismatch in thermal expansion between eGaIn and gallium oxide.[8–12] Since both of these activation strategies require relatively long processing times, a need remains for an ultrafast sintering method that is compatible with high-throughput additive manufacturing. Rapid photonic sintering, which is achieved using an intense

S. G. Wallace, N. P. Bradshaw, N. X. Williams, J. H. Qian
Department of Materials Science and Engineering
Northwestern University
Evanston, IL 60208, USA
K. W. Putz
Department of Materials Science and Engineering
SURVICE Engineering
Supporting the Army Research Lab, Impact Physics Branch
Northwestern University
Evanston, IL 60208, USA
C. E. Tabor
Materials and Manufacturing Directorate
Air Force Research Laboratory
Wright Patterson AFB, OH 45433, USA
M. C. Hersam
Department of Chemistry
Department of Electrical and Computer Engineering
Department of Materials Science and Engineering
Northwestern University
Evanston, IL 60208, USA
E-mail: m-hersam@northwestern.edu
The ORCID identification number(s) for the author(s) of this article can be found under https://doi.org/10.1002/admt.202101178.

DOI: 10.1002/admt.202101178

pulsed light (IPL) flash lamp, is a rapid, noncontact technique that has been previously employed for other printed electrical conductors. For example, IPL is widely used to heat printed metallic nanoparticles (e.g., silver or copper nanoparticles) without damaging the underlying substrate during sintering.[18–25] In contrast to laser sintering that requires raster scanning across the substrate, IPL exposes a large area at once, making IPL ideal for high-throughput roll-to-roll manufacturing. In addition to metallic nanoparticles, IPL has also been used to process other electrically conductive materials such as graphene mixed with cellulosic polymers,[26,27] suggesting that IPL can be applied to other solution-processed electrical conductors, such as eGaIn nanoparticles, once suitable polymer additives are identified.

Here, we explore IPL flash lamp sintering of spray-coated eGaIn nanoparticle films. While optimized IPL conditions can directly lead to the formation of electrically conductive eGaIn films, the addition of the polymer nitrocellulose provides additional combustion energy to further enhance the electrical conductivity by another 60%, ultimately resulting in IPL-activated eGaIn nanoparticle films with electrical conductivities exceeding 10^4 S cm^{-1}. The nitrocellulose additive provides additional benefits through enhanced colloidal stability to eGaIn nanoparticle dispersions, which minimizes eGaIn nanoparticle aggregation preceding deposition into thin films. Most significantly, combustion-assisted photonic sintering (CAPS) of eGaIn nanoparticle films is two orders of magnitude faster than previously demonstrated noncontact sintering techniques. In this manner, CAPS provides a pathway for eGaIn nanoparticles to be utilized in high-throughput additive manufacturing of flexible electronics.

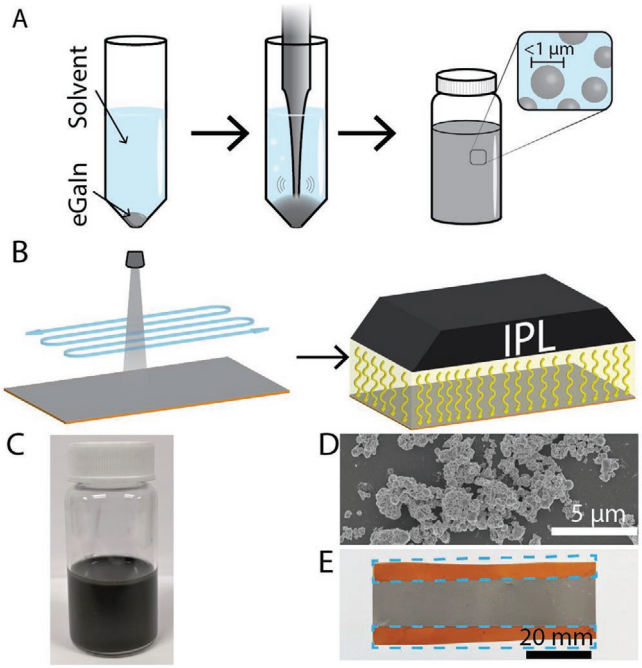

Figure 1. eGaIn spray coating. A) Schematic representation of eGaIn nanoparticle inks, produced through horn sonication in acetonitrile. B) Spray coating eGaIn ink with a constant raster motion across the substrate prevents wet solvent from pooling before exposure to IPL for photonic sintering. C) Photograph of the eGaIn nanoparticle ink. D) Scanning electron microscopy image of the eGaIn nanoparticles. E) Example of a physically masked (dashed rectangles), spray-coated eGaIn nanoparticle film on a flexible polyimide substrate.

2. Results and Discussion

Nanoparticle-based eGaIn dispersions were formed by tip sonication in acetonitrile (**Figure 1**A).[28] These inks were then spray coated onto a polyimide substrate with a constant raster motion to achieve an even coating of approximately 8 ± 1 µm in thickness across all films preceding exposure to the IPL flash lamp (Figure 1B). Spray coating is a roll-to-roll compatible deposition process in which a continuous stream of aerosolized ink droplets is propelled towards a surface by means of pressurized air and can be used to rapidly obtain uniform films of nanoparticles.[29] A photograph of the dispersed ink is provided in Figure 1C, with an electron microscopy image of the as-printed eGaIn nanoparticles shown in Figure 1D. When spray coated, an evenly coated eGaIn nanoparticle film is obtained (Figure 1E).

Polyimide is chosen as the substrate in this study due to its ubiquity in flexible electronics and roll-to-roll processing as well as its chemical, thermal, and mechanical stability. After spray coating the eGaIn nanoparticle ink on polyimide, the resulting eGaIn nanoparticle film is exposed to IPL to induce photonic sintering. Following millisecond-scale IPL exposure, the film transitions from electrically insulating to electrically conductive (schematic shown in inset of **Figure 2**A). To obtain the dependence of the resulting electrical conductivity on IPL exposure conditions, multiple films were exposed to IPL pulse energies in the range of 1–7 J cm^{-2}. After IPL exposure, the electrical conductivity of each film was measured, and the average value and standard deviation were plotted as a function of exposure energy (Figure 2A). The maximum average electrical conductivity of ≈6 600 S cm^{-1} was achieved following an IPL exposure of 6 J cm^{-2}. IPL sintering was unable to induce rupture of the gallium oxide shells around the eGaIn nanoparticles at IPL energies below 5 J cm^{-2}, as evidenced by the negligible electrical conductivity following these IPL exposure conditions. On the other hand, at an IPL energy of 7 J cm^{-2}, the electrical conductivity decreases from the 6 J cm^{-2} peak due to increased film damage caused by excessive IPL energy. This film damage is similar to the effect observed in previously reported laser sintering studies where eGaIn nanoparticles were ablated at high laser intensities.[11] For the optimal IPL exposure condition of 6 J cm^{-2}, scanning electron microscopy (SEM) reveals extensive rupture of the gallium oxide shells and resulting coalescence of eGaIn nanoparticles into larger microparticles that ultimately form a continuous LM network that provides electrically conductive pathways throughout the film (Figure 2B). This coalescence phenomenon has been observed in other LM particle systems that were mechanically sintered.[17] The light-colored particulates that are apparent in the SEM images are likely remnants of the shattered gallium oxide shells leftover from the ruptured eGaIn nanoparticles.

While IPL on films consisting of eGaIn nanoparticles alone can reach an electrical conductivity approaching ≈20% of bulk eGaIn (34 000 S cm^{-1}),[11] the continued presence of spherical

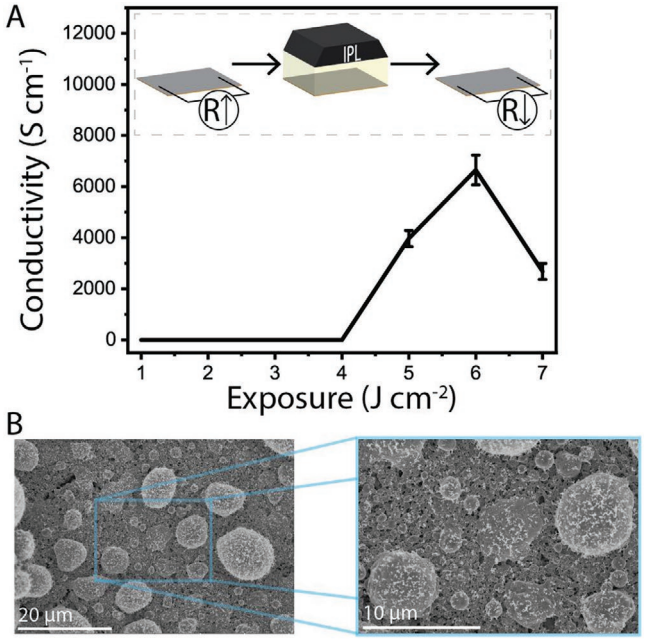

Figure 2. Electrical characterization and SEM of IPL-exposed eGaIn films. A) Electrical conductivity of spray-coated eGaIn nanoparticle films as a function of IPL exposure. The maximum electrical conductivity 6,650 S cm^{-1} is found following an IPL exposure of 6 J cm^{-2}, $n = 3$ samples are plotted at each point. B) Scanning electron microscopy images of the surface of the spray-coated eGaIn nanoparticle film after the optimal IPL exposure of 6 J cm^{-2}. Photonic sintering fractures the gallium oxide shells and drives coalescence of the eGaIn nanoparticles into larger microparticles that ultimately form a continuous electrically conductive network.

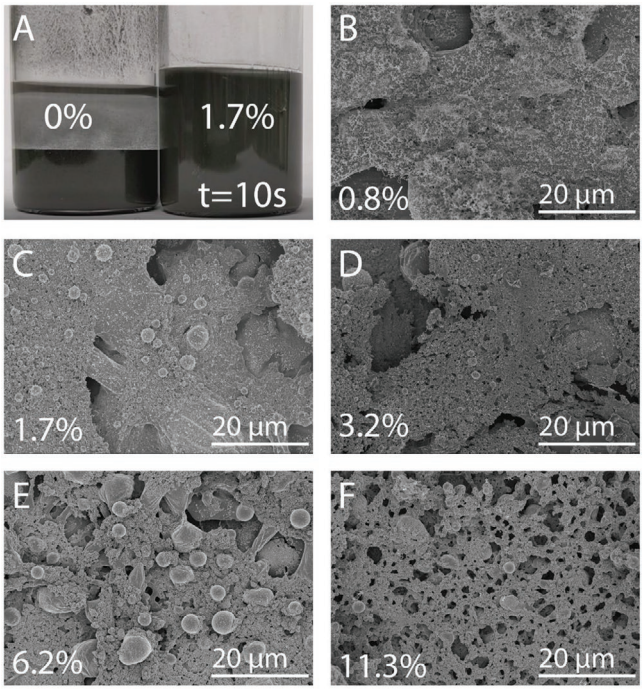

Figure 3. Demonstration of colloidal stability and SEM of IPL-exposed eGaIn-NC films. A) NC leads to improved stability of eGaIn nanoparticle dispersions. In particular, eGaIn nanoparticle dispersions with 0 wt% NC and 1.7 wt% NC inks were mixed with ten seconds of hand shaking, and then a photograph was taken after ten seconds of settling. The accompanying video is available in the Supporting Information. (B–F) Scanning electron microscopy images of the eGaIn nanoparticle films with 0.8 wt%, 1.7 wt%, 3.2 wt%, 6.2 wt%, and 11.3 wt% NC films after curing at 6 J cm^{-2}.

unruptured eGaIn nanoparticles up to the point of film ablation suggests that an additional sintering mechanism is needed that can supplement IPL. In particular, since the mechanical rupture force of eGaIn nanoparticles is size dependent, an alternative energy source would ideally assist in sintering the distribution of particle sizes observed in Figure 1D.[30,31] Toward this end, nitrocellulose was employed as a chemically energetic polymer additive to provide an additional sintering path for the eGaIn nanoparticle film when triggered by IPL. Nitrocellulose (NC) is a nitrated cellulosic polymer derivative that combusts exothermically and has proven to be effective at dispersing nanomaterials and producing uniform films.[32–34] As shown in Figure 3A, nitrocellulose also provides a significant improvement in dispersion stability compared to polymer-free eGaIn nanoparticle dispersions. Whereas polymer-free eGaIn nanoparticles rapidly settle out of dispersion within 10 s, the incorporation of 1.7 wt% NC maintains a homogeneous eGaIn nanoparticle dispersion for at least 24 h. Supporting Video 1 compares eGaIn nanoparticle dispersions with and without NC, clearly showing the improvement in dispersion stability with NC.

To explore the effects of nitrocellulose on eGaIn nanoparticle films, a series of NC/eGaIn dispersions with varying NC concentrations was prepared. In all cases, the NC was added to the dispersion after eGaIn nanoparticle formation. The same procedure was performed to generate the eGaIn nanoparticles, resulting in the identical base eGaIn concentration and total weight of eGaIn in each dispersion. Since each print consumed the entirety of the dispersion, the resulting thin films contained the same mass of eGaIn with varying ratios of eGaIn to NC. These NC/eGaIn dispersions were spray coated onto polyimide substrates and IPL sintered using the same process as the NC-free eGaIn nanoparticle dispersions. Even at the highest NC loading of 11.3 wt%, no phase segregation was observed between the eGaIn nanoparticles and the NC in the as-deposited films (Figure S1, Supporting Information).

After spray coating, the films were then exposed to the same range of IPL energies as the baseline ink. SEM images of these films at 6 J cm^{-2} IPL exposure are shown in **Figure 3**. The 0.8 wt% and 1.7 wt% NC film compositions (Figure 3 B,C) showed the formation of larger coalesced structures that led to improved electrical conductivity. Increasing damage to the film can be seen at higher NC concentrations (Figure 3D–F). This damage occurs in the form of increased porosity of the IPL-sintered film, which culminates in the lacey structure of the 11.3 wt% NC film shown in Figure 3F. Despite the potential for self-propagation of IPL-triggered NC combustion, masking of the IPL-exposed area results in patterned eGaIn conductive traces (Figure S2, Supporting Information). Additionally, the energetic combustion process does not redistribute conductive particles onto the surrounding polyimide (Figure S3, Supporting Information). Furthermore, the conditions experienced

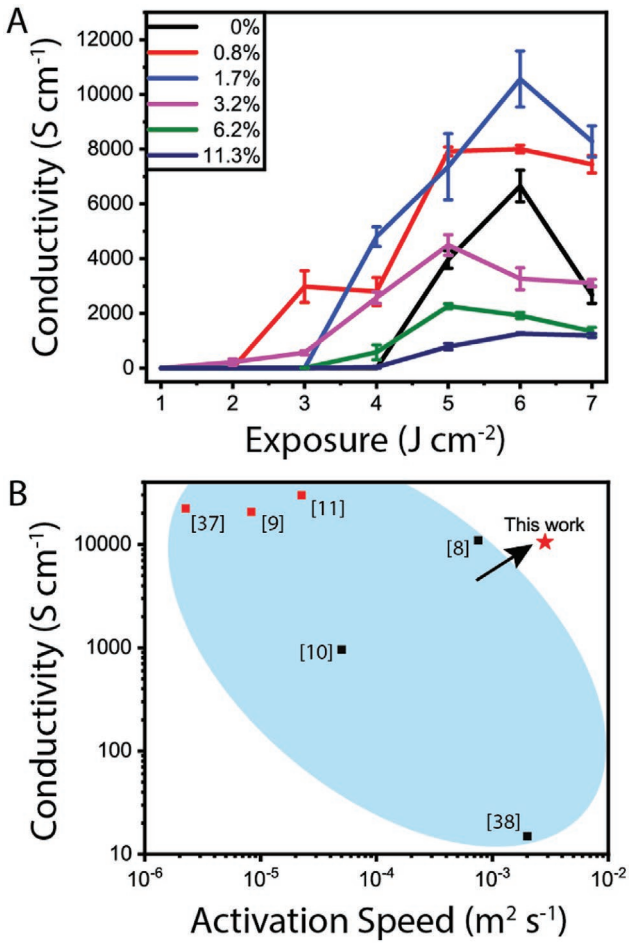

Figure 4. Electrical characterization and activation speed comparison of IPL-exposed NC/eGaIn films. A) Electrical conductivity of the six different NC/eGaIn ink compositions (including the previously shown 0 wt% NC ink) as a function of IPL energies. The maximum electrical conductivity was achieved at an IPL exposure of 6 J cm^{-2} for 1.7 wt% NC composition. $n = 3$ samples are plotted at each point. B) Benchmarking plot of maximum electrical conductivity versus eGaIn nanoparticle activation speed for previously published eGaIn nanoparticle films. Noncontact and mechanical activation techniques are labeled in red and black, respectively.

by the underlying polyimide during the combustion process did not lead to measurable substrate damage.

Charge transport measurements were then performed to assess the electrical conductivity of the IPL-sintered NC/eGaIn films. Consistent with the SEM images showing interconnected eGaIn domains, both the 0.8 wt% and 1.7 wt% NC films possessed increased electrical conductivity compared to the NC-free film (**Figure 4**A), indicating that the additional gallium oxide shell rupture induced by IPL-triggered NC combustion enhances charge transport. As was the case with NC-free films, the best performing NC/eGaIn films have peak electrical conductivities following IPL sintering at 6 J cm^{-2}. The 1.7 wt% NC film produced the maximum average electrical conductivity of ≈10 560 S cm^{-1}, which is a 60% increase over the maximum average electrical conductivity in the NC-free films. Increased film damage from excessive energetic NC decomposition leads to a corresponding decrease in electrical conductivity for the high-NC-content films (NC concentrations >1.7 wt%). SEM images for the full IPL range of 1–7 J cm^{-2} are provided for the 1.7 wt% NC films in Figure S3, Supporting Information.

At 6 J cm^{-2}, the IPL source used in this study evenly exposed 25 cm^2 areas. However, larger IPL sources are commercially available, and thus this technique can be readily scaled to enable high-throughput roll-to-roll processing, which typically occurs at web speeds of ≈0.2 m s^{-1} for flexible electronics and photovoltaics.[35] Furthermore, due to the parallel nature of CAPS, it could be straightforwardly scaled up through the use of larger IPL exposure units, making it compatible with inline integration for higher speed roll-to-roll techniques such as gravure printing of low viscosity inks, which can reach speeds of 15 m s^{-1}.[36]

Compared to other printed eGaIn nanoparticle activation techniques, CAPS is faster in activation speed, while still maintaining a high electrical conductivity exceeding 10^4 S cm^{-1}. To achieve this electrical conductivity, a 1.7 ms duration IPL pulse with an instrument recharge time of 875 ms between pulses was used, resulting in an areal activation rate of 2.85×10^{-3} m^2 s^{-1}. While alternative parallel processing techniques like stamping could be further scaled up to increase areal activation speed, large-area stamping has not yet been demonstrated and IPL can similarly be scaled up while maintaining a faster activation speed per area. A benchmarking comparison plot for electrical conductivity and activation speed is shown in Figure 4B, with further details provided in Table S1, Supporting Information. The CAPS method demonstrated here is two orders of magnitude faster than other non-contact techniques such as laser writing[11,37] and furnace heating.[38] As further comparison, the conductivity and activation speed compare favorably with the mechanical activation techniques of stretching,[8] stamping,[9] and stylus writing.[10] While the speed and electrical performance of CAPS is similar to that demonstrated by a stretching-based technique,[8] stretching is incompatible with roll-to-roll processing, which typically requires constant web tension.[39] Similar to other parallel processing techniques like stamping, CAPS can be further scaled to higher speeds using larger or more rapid commercially available IPL sources, thus making this method highly amenable to roll-to-roll manufacturing.

3. Conclusion

In summary, ultrafast millisecond-scale IPL photonic sintering of eGaIn nanoparticle thin films has been demonstrated. While IPL alone can fracture the gallium oxide shell of eGaIn nanoparticles to achieve electrical conductivities approaching ≈20% of the bulk eGaIn value, further improvements can be achieved through the incorporation of energetic NC. In particular, the IPL-triggered exothermic decomposition of NC results in eGaIn nanoparticle thin films with electrical conductivities exceeding 10^4 S cm^{-1}. This CAPS process is two orders of magnitude faster than previously demonstrated noncontact sintering techniques. By overcoming the traditional tradeoff between processing speed and electrical conductivity, CAPS processing provides a scalable pathway to employing eGaIn nanoparticle

inks in high-throughput roll-to-roll manufacturing of printable and flexible electronics.

4. Experimental Section

Liquid Metal Dispersions: Indium shot and gallium (Sigma-Aldrich) were mixed together to create a 22 wt% indium alloy. Heating at 80 °C was used to melt the pure metals and aid in alloying. A mass of 800 mg of the resulting alloy was transferred via syringe to a conical centrifuge tube, followed by 10 ml of acetonitrile (Sigma-Aldrich). Tip sonication with a 1/8th inch sonication tip and 12 W of sonication power (Fisher Scientific Sonic Dismembrator Model 500, 30%, 1 h) was then used to create the final dispersion containing eGaIn nanoparticles encapsulated with gallium oxide shells.

Nitrocellulose-Acetonitrile Solution: Nitrocellulose powder (5–6 sec, Scientific Polymer) was dissolved in acetonitrile (Sigma-Aldrich) to a concentration of 20 mg ml^{-1}. The powder is 68 wt% nitrocellulose, damped with isopropanol.

Spray Coating: A volume of 10 ml liquid metal dispersion and a corresponding volume of nitrocellulose-acetonitrile solution required to obtain the desired nitrocellulose:eGaIn ratio were mixed together by bath sonication. After mixing, the dispersion density was found to be 861 ± 2 mg ml^{-1} with no significant difference based on the NC loading. Without nitrocellulose, the inks were found to have a viscosity of 2.3 mPa-s, which increased up to 2.7 mPa-s with 1.7 wt% NC loading. The dispersion was spray coated onto polyimide substrates with a gravity feed spray gun (TCP Global F3-SET, 1.0 mm nozzle) at a distance of approximately 15 cm and at a pressure of approximately 150 kPa. This spray coating was performed at a translation speed of approximately 10 cm s^{-1}.

Photonic Sintering: A Xenon S-2100 flash lamp was used to expose samples to IPL pulses with pulse energies of 1–7 J cm^{-2}. The flash lamp voltage was set at 3 kV, and the pulse width was modulated from 0.3 to 2 ms to achieve the different pulse energies. Single pulses were applied, and samples were held at a distance of 25 mm from the flash lamp.

Electrical Characterization: Electrical measurements of the spray-coated films were performed with a Keithley source meter attached to an inline 4-point probe measurement system. Appropriate geometric correction factors were employed to extract the electrical conductivity. The thicknesses of each individual film were obtained with an Olympus OLS5000 laser confocal microscope. Step height between the polyimide substrate and the top of the spray-coated film was measured with a 20*x* objective. Olympus software was used to analyze the data and find the average height difference between a cleared area and a nearby area of the spray-coated film near the point of electrical contact for the four-point probe. Additionally, double stick tape was used to maintain film flatness during measurement.

Scanning Electron Microscopy: The spray-coated eGaIn nanoparticle films were adhered with carbon tape to scanning electron microscopy mounts, and then each sample was coated with 7 nm of Os (SPI Osmium Coater, with OsO_4 as a volatile source) to create a conformal conductive coating prior to imaging. Images were collected with a Hitachi SU8030 scanning electron microscope with an accelerating voltage of 5 kV.

Statistical Analysis: For each pairing of nitrocellulose loading and IPL exposure, the average and standard deviation of electrical conductivity of $n = 3$ samples were plotted. If samples were obvious outliers due to a >50% difference in electrical conductivity from the average, they were replaced. These outliers typically occurred from problems in measuring thickness or damage to the samples.

Supporting Information

Supporting Information is available from the Wiley Online Library or from the author.

Acknowledgements

This work was supported by the Air Force Research Laboratory under agreement number FA8650-15-2-5518. This work made use of the MatCI Facility that is supported by the MRSEC program of the National Science Foundation (DMR-1720139) at the Materials Research Center of Northwestern University. In addition, this work made use of the NUFAB facility of the Northwestern University NUANCE Center, which has received support from the SHyNE Resource (NSF ECCS-2025633), the IIN, and the Northwestern MRSEC program (NSF DMR-1720139). The U.S. Government is authorized to reproduce and distribute reprints for Governmental purposes notwithstanding any copyright notation thereon. The views and conclusions contained herein are those of the authors and should not be interpreted as necessarily representing the official policies or endorsements, either expressed or implied, of the sponsors.

Conflict of Interest

The authors declare no conflict of interest.

Data Availability Statement

The data that support the findings of this study are available from the corresponding author upon reasonable request.

Keywords

eutectic gallium-indium alloy, eGaIn, intense pulsed light, photonic sintering, flexible electronics

Received: September 7, 2021
Revised: October 14, 2021
Published online: November 2, 2021

[1] Y. Ding, X. Guo, Y. Qian, L. Xue, A. Dolocan, G. Yu, *Adv. Mater.* **2020**, *32*, 2002577.
[2] G. J. Hayes, J. H. So, A. Qusba, M. D. Dickey, G. Lazzi, *IEEE Trans. Antennas Propag.* **2012**, *60*, 2151.
[3] M. D. Dickey, *Adv. Mater.* **2017**, *29*, 1606425.
[4] J. W. Boley, E. L. White, G. T. C. Chiu, R. K. Kramer, *Adv. Funct. Mater.* **2014**, *24*, 3501.
[5] Y. Lin, O. Gordon, M. R. Khan, N. Vasquez, J. Genzer, M. D. Dickey, *Lab Chip* **2017**, *17*, 3043.
[6] M. D. Dickey, R. C. Chiechi, R. J. Larsen, E. A. Weiss, D. A. Weitz, G. M. Whitesides, *Adv. Funct. Mater.* **2008**, *18*, 1097.
[7] M. Kim, D. K. Brown, O. Brand, *Nat. Commun.* **2020**, *11*, 1002.
[8] B. Yao, W. Hong, T. Chen, Z. Han, X. Xu, R. Hu, J. Hao, C. Li, H. Li, S. E. Perini, M. T. Lanagan, S. Zhang, Q. Wang, H. Wang, *Adv. Mater.* **2020**, *32*, 1907499.
[9] R. Abbasi, M. Mayyas, M. B. Ghasemian, F. Centurion, J. Yang, M. Saborio, F. M. Allioux, J. Han, J. Tang, M. J. Christoe, K. M. Mohibul Kabir, K. Kalantar-Zadeh, M. A. Rahim, *J. Mater. Chem. C* **2020**, *8*, 7805.
[10] Y. Lin, C. Cooper, M. Wang, J. J. Adams, J. Genzer, M. D. Dickey, *Small* **2015**, *11*, 6397.
[11] S. Liu, M. C. Yuen, E. L. White, J. W. Boley, B. Deng, G. J. Cheng, R. Kramer-Bottiglio, *ACS Appl. Mater. Interfaces* **2018**, *10*, 28232.

[12] S. Liu, S. N. Reed, M. J. Higgins, M. S. Titus, R. Kramer-Bottiglio, *Nanoscale* **2019**, *11*, 17615.
[13] M. G. Mohammed, R. Kramer, *Adv. Mater.* **2017**, *29*, 1604965.
[14] J. W. Boley, E. L. White, R. K. Kramer, *Adv. Mater.* **2015**, *27*, 2355.
[15] D. Zrnic, D. S. Swatik, *J. Less-Common Met.* **1969**, *18*, 67.
[16] Z. J. Farrell, C. Tabor, *Langmuir* **2018**, *34*, 234.
[17] C. J. Thrasher, Z. J. Farrell, N. J. Morris, C. L. Willey, C. E. Tabor, *Adv. Mater.* **2019**, *31*, 1903864.
[18] M. Hösel, F. C. Krebs, *J. Mater. Chem.* **2012**, *22*, 15683.
[19] Y. Galagan, E. W. C. Coenen, R. Abbel, T. J. Van Lammeren, S. Sabik, M. Barink, E. R. Meinders, R. Andriessen, P. W. M. Blom, *Org. Electron.* **2013**, *14*, 38.
[20] Y. Oh, I. S. Yoon, C. Lee, S. H. Kim, B. K. Ju, J. M. Hong, *J. Mater. Chem. C* **2017**, *5*, 11733.
[21] J. Niittynen, E. Sowade, H. Kang, R. R. Baumann, M. Mäntysalo, *Sci. Rep.* **2015**, *5*, 2.
[22] H. S. Kim, S. R. Dhage, D. E. Shim, H. T. Hahn, *Appl. Phys. A* **2009**, *97*, 791.
[23] J. Ryu, H. S. Kim, H. T. Hahn, *J. Electron. Mater.* **2011**, *40*, 42.
[24] G. Polino, S. Shanmugam, G. J. P. Bex, R. Abbel, F. Brunetti, A. Di Carlo, R. Andriessen, Y. Galagan, *ACS Appl. Mater. Interfaces* **2016**, *8*, 2325.
[25] M. Zenou, O. Ermak, A. Saar, Z. Kotler, *J. Phys. D:S Appl. Phys.* **2014**, *47*, 025501.
[26] E. B. Secor, B. Y. Ahn, T. Z. Gao, J. A. Lewis, M. C. Hersam, *Adv. Mater.* **2015**, *27*, 6683.
[27] E. B. Secor, T. Z. Gao, M. H. Dos Santos, S. G. Wallace, K. W. Putz, M. C. Hersam, *ACS Appl. Mater. Interfaces* **2017**, *9*, 29418.
[28] J. N. Hohman, M. Kim, G. A. Wadsworth, H. R. Bednar, J. Jiang, M. A. Lethai, P. S. Weiss, *Nano Lett.* **2011**, *11*, 5104.
[29] R. R. Søndergaard, M. Hösel, F. C. Krebs, *J. Polym. Sci., Part B: Polym. Phys.* **2013**, *51*, 16.
[30] N. J. Morris, Z. J. Farrell, C. E. Tabor, *Nanoscale* **2019**, *11*, 17308.
[31] T. R. Lear, S. H. Hyun, J. W. Boley, E. L. White, D. H. Thompson, R. K. Kramer, *Extrem. Mech. Lett.* **2017**, *13*, 126.
[32] E. B. Secor, T. Z. Gao, A. E. Islam, R. Rao, S. G. Wallace, J. Zhu, K. W. Putz, B. Maruyama, M. C. Hersam, *Chem. Mater.* **2017**, *29*, 2332.
[33] F. Sullivan, L. Simon, N. Ioannidis, S. Patel, Z. Ophir, C. Gogos, M. Jaffe, S. Tirmizi, P. Bonnett, P. Abbate, *AIChE J.* **2020**, *66*, e16234.
[34] L. N. Jimenez, C. D. V. M. Narváez, C. Xu, S. Bacchi, V. Sharma, in *Surface Science and Adhesion Cosmetics*, Wiley, New York **2021**.
[35] M. Hösel, R. R. Søndergaard, M. Jørgensen, F. C. Krebs, *Energy Technol.* **2013**, *1*, 102.
[36] R. Søndergaard, M. Hösel, D. Angmo, T. T. Larsen-Olsen, F. C. Krebs, *Mater. Today* **2012**, *15*, 36.
[37] T. Lu, E. J. Markvicka, Y. Jin, C. Majidi, *ACS Appl. Mater. Interfaces* **2017**, *9*, 22055.
[38] S. Liu, D. S. Shah, R. Kramer-Bottiglio, *Nat. Mater.* **2021**, *20*, 851.
[39] D. Feng, R. B. Wagner, A. Raman, *Flexible Printed Electron.* **2021**, *6*, 035006.